

# Motion-Compensated Coding and Frame-Rate Up-Conversion: Models and Analysis

Yehuda Dar and Alfred M. Bruckstein

Technion – Israel Institute of Technology  
Haifa 32000, Israel

E-mail: ydar@tx.technion.ac.il, freddy@cs.technion.ac.il

## Abstract

Block-based motion estimation (ME) and compensation (MC) techniques are widely used in modern video processing algorithms and compression systems. The great variety of video applications and devices results in numerous compression specifications. Specifically, there is a diversity of frame-rates and bit-rates. In this paper, we study the effect of frame-rate and compression bit-rate on block-based ME and MC as commonly utilized in inter-frame coding and frame-rate up conversion (FRUC). This joint examination yields a comprehensive foundation for comparing MC procedures in coding and FRUC. First, the video signal is modeled as a noisy translational motion of an image. Then, we theoretically model the motion-compensated prediction of an available and absent frames as in coding and FRUC applications, respectively. The theoretic MC-prediction error is further analyzed and its autocorrelation function is calculated for coding and FRUC applications. We show a linear relation between the variance of the MC-prediction error and temporal-distance. While the affecting distance in MC-coding is between the predicted and reference frames, MC-FRUC is affected by the distance between the available frames used for the interpolation. Moreover, the dependency in temporal-distance implies an inverse effect of the frame-rate. FRUC performance analysis considers the prediction error variance, since it equals to the mean-squared-error of the interpolation. However, MC-coding analysis requires the entire autocorrelation function of the error; hence, analytic simplicity is beneficial. Therefore, we propose two constructions of a separable autocorrelation function for prediction error in MC-coding. We conclude by comparing our estimations with experimental results.

# 1 Introduction

Temporal redundancy is a main property of video signals. This redundancy originates in the similarity between successive frames in a video scene. Moreover, a video scene can be thought of as a composition of static and moving regions. Therefore, many video compression and processing systems utilize motion estimation (ME). Ideally, the motion should be estimated per pixel; however, practical systems have run-time limitations, and therefore cannot apply estimation per pixel. Hence, block-based ME techniques are widely used in practical video compression and processing algorithms. Block-based ME is the procedure of estimating block motion by comparing it with blocks in a search area within another frame in the sequence. This method approximates the motion as translational, and represents it by a motion-vector and reference frame indication.

In block-based hybrid compression, ME is utilized for inter-frame prediction of a coded block. Motion-compensation (MC) is the subtraction between the coded block and its prediction. This results in the block's prediction error, also known as the MC-residual. The MC-residual is further coded and sent to the decoder. Therefore, the MC-residual greatly affects the performance of inter-frame coding. Furthermore, due to the extensive use of inter-frame coding, the MC-residual also significantly influences the overall compression performance.

Accordingly, the MC-residual has been widely studied since the 1980's [1–12]. However, these studies have not explicitly considered the frame-rate effect on the MC-residual statistics. Moreover, only Guo et al. [10] mentioned the influence of frame-reconstruction quality (and, therefore, bit-rate) on the MC-residual. In this paper, we analyze the effects of frame-rate (through the temporal-distance) and bit-rate on the MC-residual autocorrelation function. Most of the available analytic models are too complex for being a basis for analysis of an entire compression system. Here we propose two models for the autocorrelation. First, we derive a rather complex expression from our theoretic model for MC-prediction of an available frame (i.e., as in coding). Then, we simplify the autocorrelation to a separable form similar to [11] and [5]. Furthermore, we justify our analysis by experimental observations.

Frame-rate up conversion (FRUC) is the procedure of increasing the frame-rate of a video by temporal interpolation of frames. There are several motivations for using FRUC. It is used for video format conversion when the target format has higher frame-rate. In addition, high frame-rates were found to increase the subjective quality [13]; therefore, some applications may apply FRUC on low frame-rate videos. Another application of FRUC is for improving low bit-rate video coding as follows: the frame-rate is reduced before compression, and increased back to its original value after the reconstruction of the compressed data. As a result, the output video quality is improved for a constant bit-budget.

FRUC algorithms trade off between computational complexity and the quality of the interpolated frames. Simple FRUC techniques disregard the motion in the sequence, e.g., interpolating by frame repetition or averaging. For non-static regions, this results in motion jerkiness and ghost artifacts. Therefore, the com-

monly used interpolation techniques consider motion. Specifically, methods that utilize motion-trajectory estimation are known as motion-compensated FRUC (MC-FRUC).

Some studies have proposed complex FRUC algorithms that try to accurately model the motion in the video, e.g., [14]. However, high computational complexity limits these algorithms for offline usage, whereas some applications require real-time FRUC. A reasonable computational complexity is achieved in block-based MC-FRUC techniques; therefore, they are widely used and studied [15–19]. Block-based MC-FRUC is usually performed by applying block-matching procedure between existing frames, resulting in a trajectory of the estimated translational motion; then, this motion-trajectory is used for interpolating missing blocks according to the applied method [15–19].

In [19], the MC-FRUC error was analyzed in the power-spectral-density (PSD) domain and by using a statistical model of the motion-vector error. They searched for the optimal temporal filter. In this paper, we study the block-based MC-FRUC error in the pixel domain. The examined procedure models low-complexity methods (e.g., [15]), which are commonly used. Consequently, the proposed analytic derivations are relatively simple.

Block-based ME differs from the true motion by assuming it is translational. This sub-optimality has minor importance in the application of MC for inter-frame coding, where the motion estimation is performed at the encoder between two accessible frames, and the target is minimal prediction residual. However, ME in FRUC aims at estimating the true motion in a missing frame. Therefore, the translational motion assumption deteriorates MC-FRUC performance. Dane and Nguyen [19] discussed the differences between the application of MC to coding and FRUC. This paper continues this examination by giving side by side analyses of MC-coding and MC-FRUC, which are easily comparable due to joint assumptions and mathematical tools.

This paper is organized as follows. In section 2, we present a theoretic model for the video signal. Section 3 analyzes the MC-prediction and its error for the cases of available and absent frames, i.e., coding and FRUC, respectively. Section 4 introduces two constructions of a separable autocorrelation function for MC-coding. In section 5 we study the theoretic estimations of our model. In section 6 we present experimental results to validate our models. Section 7 concludes this paper.

## 2 Video Signal Model

### 2.1 A Noised Translational Motion Model

The digital video signal is a temporal sequence of 2D images, i.e.  $\{f_t(x, y)\}_{t=0}^T$ . Adjacent frames are known to be correlated; hence, we relate the frames by assuming a translational motion of a 2D image with additive noise process.

We assume that the frame sequence  $\{f_t(x, y)\}_{t=0}^T$  is decomposable into two sequences. First, a 2D image with a translational motion denoted as

$\{v_t(x, y)\}_{t=0}^T$ . Second, a temporally-accumulated noise process,  $\{n_t(x, y)\}_{t=0}^T$ , that represents differences between  $\{v_t(x, y)\}_{t=0}^T$  and the actual frames due to deviations from translational motion such as deformations of objects, camera noise and quantization noise. The proposed decomposition is expressed as follows.

$$f_t(x, y) = v_t(x, y) + n_t(x, y) \quad (1)$$

The underlying translational motion process is defined as follows. The motion at the  $t^{th}$  frame relative to its predecessor at  $t-1$  is denoted as  $\varphi(t, t-1) = (\varphi_x(t, t-1), \varphi_y(t, t-1))$ . Hence, the motion in the video can be represented by the sequence  $\{\varphi(i, i-1)\}_{i=1}^T$ . Moreover, the motion between two time points,  $t_1$  and  $t_2$ , is defined as follows.

$$\varphi(t_2, t_1) = \begin{cases} \sum_{i=t_1+1}^{t_2} \varphi(i, i-1) & , \text{ for } t_1 < t_2 \\ - \sum_{i=t_2+1}^{t_1} \varphi(i, i-1) & , \text{ for } t_2 < t_1 \\ (0, 0) & , \text{ for } t_1 = t_2 \end{cases} \quad (2)$$

We model  $v_t$  to be a constant base frame,  $v$ , spatially shifted by  $(\varphi_x(t, 0), \varphi_y(t, 0))$ , i.e.,

$$v_t(x, y) = v(x - \varphi_x(t, 0), y - \varphi_y(t, 0)) \quad (3)$$

The image  $v$  is assumed to be wide-sense stationary (WSS) and is modeled using first-order Markov process, i.e., its autocorrelation is

$$R_v(k, l) = \sigma_v^2 \cdot \rho_v^{|k|+|l|}. \quad (4)$$

We model the noise,  $n_t$ , as a combination of two elements. Firstly, a temporally-local noise,  $w_t$ , that represents distortions that are relevant only for the frame at time  $t$ , e.g., camera noise or quantization noise. Secondly, we represent object deformations using a temporally-accumulated noise process. We assume that frames have equal average energy (i.e.,  $f_t$  has a constant variance for any  $t$ ). Therefore, there is a fixed amount of object deformation relative to the original form in  $v$ ; otherwise, the immersion of  $v$  in noise will increase over time. Consequently, the noise component,  $n_t$ , also represents the accumulated deviation from translational motion along the recent  $L$  frames; i.e., the process has finite memory of length  $L$ . For  $n_t$ 's construction, we use an auxiliary noise sequence  $\{q_t\}_{t=-L+1}^\infty$ , which is a spatially i.i.d random variable with a zero-mean Gaussian distribution with variance  $\sigma_q^2$ . Moreover,  $q_i$  is independent from  $q_k$  for  $i \neq k$ , and from  $w_j$  for any  $j$ . We assume that at each time point,  $t$ , spatial noise signals  $q_t$  and  $w_t$  are introduced and affect  $n_t$  together with the last  $L-1$  preceding  $q_k$  elements (Fig. 1), i.e.

$$n_t(x, y) = w_t(x, y) + \sum_{i=t-L+1}^t q_i(x - \varphi_x(t, i), y - \varphi_y(t, i)). \quad (5)$$

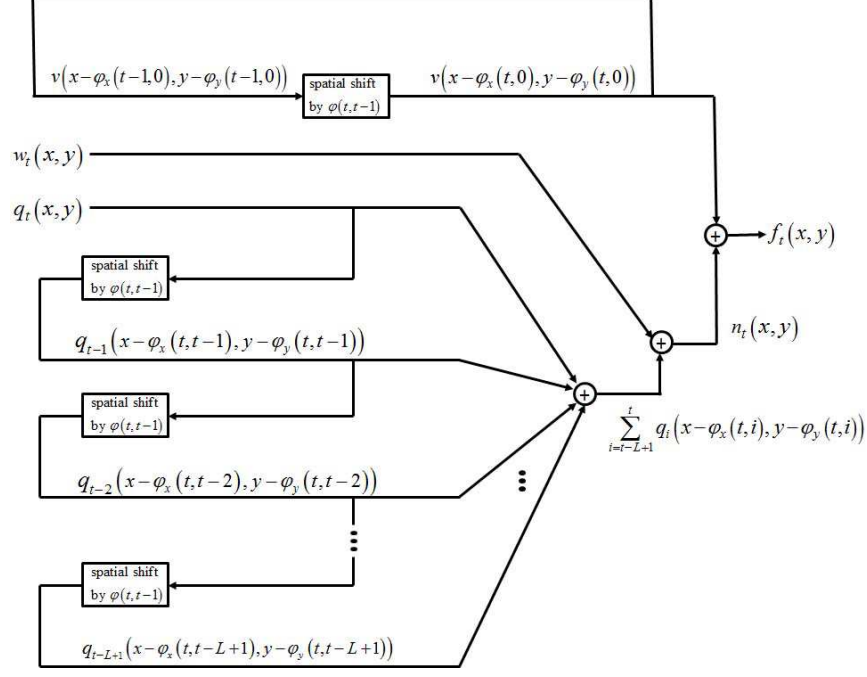


Figure 1: Demonstration of the proposed video model.

Where we utilized the property  $\varphi(t, t) = (0, 0)$ . Recall that  $q_i$  is available also for negative time points starting at  $t = -L + 1$ . Consequently, the temporally-accumulated noise has a spatially i.i.d, zero-mean Gaussian distribution with variance  $L \cdot \sigma_q^2$  for any  $t$ . Accordingly,  $n_t(x, y)$ 's autocorrelation is

$$R_{n_t}(k, l) = (\sigma_w^2 + L\sigma_q^2) \cdot \delta(k, l) \quad (6)$$

Setting (3) and (5) into (1) yields

$$\begin{aligned} f_t(x, y) &= v(x - \varphi_x(t, 0), y - \varphi_y(t, 0)) \\ &+ w_t(x, y) + \sum_{i=t-L+1}^t q_i(x - \varphi_x(t, i), y - \varphi_y(t, i)). \end{aligned} \quad (7)$$

## 2.2 Frame-Rate Effect

The variance of the auxiliary noise elements,  $\sigma_q^2$ , reflects the energy of the differences between successive frames that cannot be perfectly estimated by a translational transformation, even for a continuous images (i.e., the estimation algorithm has no spatial accuracy issues). We point here on two affecting factors: frame-rate and the compression bit-rate.

The frame-rate,  $F_{rate}$ , defines the time-intervals between successive frames to be  $\frac{1}{F_{rate}}$ . We assume that the energy of the modifications expressed in  $\sigma_q^2$  is linear in the temporal-distance. Hence,

$$\sigma_q^2 = \frac{1}{F_{rate}} \cdot \tilde{\sigma}_q^2 \quad (8)$$

Where  $\tilde{\sigma}_q^2$  is the energy of successive frames difference for a sequence of one frame per second.

## 2.3 Compression Effect

We model quality reduction due to compression as a component of the noise element  $w_t$ . This component is denoted as  $w_{t,compression}$  and it is independent with other ingredients of  $w_t$ , which their sum is denoted as  $w_{t,basic}$ . As a result,

$$\sigma_w^2 = \sigma_{w,compression}^2 + \sigma_{w,basic}^2 \quad (9)$$

where  $\sigma_{w,compression}^2$  is the variance of the compression error, i.e., the mean-squared-error (MSE).  $\sigma_{w,basic}^2$  is  $w_{t,basic}$ 's variance.

We can express  $\sigma_{w,compression}^2$  in various ways:

### 2.3.1 Empirical rate-distortion curve

$$\sigma_{w,compression}^2 = \beta \cdot r^{-\alpha} \quad (10)$$

where,  $\alpha$  and  $\beta$  are curve parameters, and  $r$  is the bit-rate.

### 2.3.2 Theoretical rate-distortion estimation for memoryless Gaussian source

A simple theoretical estimation is available under the following assumptions. Firstly, The compression distortion is similar to the procedure of directly compressing the frame pixels. Secondly, the frame pixels originated at a memoryless Gaussian source. The estimation is given by

$$\sigma_{w,compression}^2 = \sigma_v^2 \cdot 2^{-2r}, \quad (11)$$

where,  $\sigma_v^2$  is the variance of the Gaussian source, and  $r$  is the bit-rate.

### 2.3.3 Given a value that is externally known or estimated

$$\sigma_{w,compression}^2 = MSE_{compression}. \quad (12)$$

### 2.3.4 Uncompressed video

An uncompressed video has no compression error, i.e.,  $\sigma_{w,compression}^2 = 0$ ; hence,  $\sigma_w^2 = \sigma_{w,basic}^2$ .

### 3 Analysis of Motion-Compensated Prediction

In this section we analyze the two common cases of applying motion-compensation. First, we consider MC-prediction between a pair of available frames, as in MC-coding. Then, we study the case of applying MC-prediction between an existing and absent frames, as in MC-FRUC.

Our analysis is statistical, therefore we can differ from practical MC-prediction as follows. First, we treat a single MC procedure for a given signal properties, since it is statistically representative. Second, we assume it is statistically allowed to consider signals as functions without explicit spatial boundaries, although a practical MC-prediction has defined dimensions for block and search areas.

#### 3.1 MC-Prediction of an Available Frame

Let us consider the MC-prediction of frame  $f_t$  using  $f_{t-i}$  as a reference frame, where  $i \in \{0, \dots, t-1\}$ . The prediction relies on estimating the motion between  $t-i$  and  $t$  using the corresponding frames. This estimation assumes translational motion and is denoted as  $\hat{\varphi}(t, t-i | f_t, f_{t-i}) = (\hat{\varphi}_x(t, t-i | f_t, f_{t-i}), \hat{\varphi}_y(t, t-i | f_t, f_{t-i}))$ . We describe the MC-prediction as follows,

$$\begin{aligned} \hat{f}_t(x, y | f_{t-i}^{ref}, \hat{\varphi}(t, t-i | f_t, f_{t-i}^{ref})) = \\ f_{t-i}^{ref}(x - \hat{\varphi}_x(t, t-i | f_t, f_{t-i}^{ref}), y - \hat{\varphi}_y(t, t-i | f_t, f_{t-i}^{ref})) \end{aligned} \quad (13)$$

Where  $f_{t-i}^{ref}$  is a processed or distorted version of  $f_{t-i}$  that serves as a reference frame. A reference frame at time  $t$  is defined as

$$f_t^{ref}(x, y) = v_t(x, y) + n_t^{ref}(x, y). \quad (14)$$

Where, according to (5),  $n_t^{ref}$  contains  $w_t^{ref}$  that expresses the reference frame distortions. For example, real hybrid encoders utilize closed-loop MC-coding by using the reconstructed-from-compression version of  $f_{t-i}$ ; hence, we can express  $w_t^{ref}$ 's variance using (9).

We assume that

$$\hat{\varphi}(t, t-i | f_t, f_{t-i}^{ref}) \approx \hat{\varphi}(t, t-i | f_t, f_{t-i}), \quad (15)$$

i.e., compression does not affect ME accuracy significantly. Hence, (13) is modified to

$$\begin{aligned} \hat{f}_t(x, y | f_{t-i}^{ref}, \hat{\varphi}(t, t-i | f_t, f_{t-i})) = \\ f_{t-i}^{ref}(x - \hat{\varphi}_x(t, t-i | f_t, f_{t-i}), y - \hat{\varphi}_y(t, t-i | f_t, f_{t-i})). \end{aligned} \quad (16)$$

The ME is approximated using (15); however, the compression still affects the MC residual through  $\sigma_{w,compression}^2$  of the reference frame.

We assume that the object from  $f_t$ , which its motion is estimated, is contained in the search area in  $f_{t-i}$ . Therefore, we model  $\hat{\varphi}(t, t-i | f_t, f_{t-i})$  to have a displacement error  $(\Delta x, \Delta y)$  that depends only on the spatial properties of the ME algorithm, e.g., search resolution. Hence, the error excludes any temporal dependency. Specifically,

$$\begin{aligned}\hat{\varphi}_x(t, t-i | f_t, f_{t-i}) &= \varphi_x(t, t-i) + \Delta x \\ \hat{\varphi}_y(t, t-i | f_t, f_{t-i}) &= \varphi_y(t, t-i) + \Delta y\end{aligned}\quad (17)$$

Where  $\Delta x$  and  $\Delta y$  are uniformly distributed in a range defined by the accuracy of the ME algorithm. Using (1), (3) and (17) we develop (16) into

$$\begin{aligned}\hat{f}_t(x, y | f_{t-i}^{ref}, \hat{\varphi}(t, t-i | f_t, f_{t-i})) &= v(x - \varphi_x(t, 0) - \Delta x, y - \varphi_y(t, 0) - \Delta y) \\ &+ n_{t-i}^{ref}(x - \hat{\varphi}_x(t, t-i | f_t, f_{t-i}), y - \hat{\varphi}_y(t, t-i | f_t, f_{t-i})).\end{aligned}\quad (18)$$

Here we used the property  $\varphi(t, 0) = \varphi(t, t-i) + \varphi(t-i, 0)$  that follows from the definition in (2).

The MC-prediction error of  $f_t$  using  $f_{t-i}$  as a reference frame is formulated as

$$e_{t|t-i}(x, y) = f_t(x, y) - \hat{f}_t(x, y | f_{t-i}^{ref}, \hat{\varphi}(t, t-i | f_t, f_{t-i})) \quad (19)$$

In appendix A, we describe in detail the calculation of the autocorrelation function of the MC-prediction error. This derivation results in

$$\begin{aligned}R_{e_i}(k, l) &= 2(\sigma_{\Delta x}^2 + \sigma_{\Delta y}^2) \cdot [R_v(k, l) + R_{n_{t-i}^{ref}}(k, l)] \\ &- \sigma_{\Delta x}^2 \cdot [R_v(k-1, l) + R_v(k+1, l) + R_{n_{t-i}^{ref}}(k-1, l) + R_{n_{t-i}^{ref}}(k+1, l)] \\ &- \sigma_{\Delta y}^2 \cdot [R_v(k, l-1) + R_v(k, l+1) + R_{n_{t-i}^{ref}}(k, l-1) + R_{n_{t-i}^{ref}}(k, l+1)] \\ &+ R_{\Delta n_{t, t-i}}(k, l)\end{aligned}\quad (20)$$

where  $R_{\Delta n_{t, t-i}}(k, l)$  is the autocorrelation of the MC noise difference, denoted as  $\Delta n_{t_2, t_1}$  for  $t_1 < t_2$  and defines as

$$\Delta n_{t_2, t_1}(x, y) \equiv n_{t_2}(x, y) - n_{t_1}^{ref}(x - \varphi_x(t_2, t_1), y - \varphi_y(t_2, t_1)) \quad (21)$$

The following autocorrelation was calculated for  $\Delta n_{t_2, t_1}$  in the appendix (48)-(49):

$$R_{\Delta n_{t_2, t_1}}(k, l) = [2\sigma_q^2 \cdot (t_2 - t_1) + \sigma_{w_{t_1}}^2 + \sigma_{w_{t_2}}^2] \cdot \delta(k, l) \quad (22)$$

The following explicit form of (20) is provided in the appendix:

$$\begin{aligned}R_{e_i}(k, l) &= 2[\sigma_{\Delta x}^2 + \sigma_{\Delta y}^2] \cdot [\sigma_v^2 \cdot \rho_v^{|k|+|l|} + (L\sigma_q^2 + \sigma_{w, ref}^2) \cdot \delta(k, l)] \\ &- \sigma_{\Delta x}^2 \sigma_v^2 \rho_v^{|l|} \cdot [\rho_v^{|k-1|} + \rho_v^{|k+1|}]\end{aligned}\quad (23)$$



$$\begin{aligned}
& -\sigma_{\Delta x}^2 [L\sigma_q^2 + \sigma_{w,ref}^2] \cdot [\delta(k-1, l) + \delta(k+1, l)] \\
& -\sigma_{\Delta y}^2 \sigma_v^2 \rho_v^{|k|} \cdot [\rho_v^{|l-1|} + \rho_v^{|l+1|}] \\
& -\sigma_{\Delta y}^2 [L\sigma_q^2 + \sigma_{w,ref}^2] \cdot [\delta(k, l-1) + \delta(k, l+1)] \\
& + [2i\sigma_q^2 + \sigma_{w,current}^2 + \sigma_{w,ref}^2] \cdot \delta(k, l)
\end{aligned}$$

The error variance is

$$\begin{aligned}
R_{e_i}(0, 0) = & 2(\sigma_{\Delta x}^2 + \sigma_{\Delta y}^2) \cdot [\sigma_v^2 \cdot (1 - \rho_v) + (L\sigma_q^2 + \sigma_{w,ref}^2)] \\
& + 2i\sigma_q^2 + \sigma_{w,current}^2 + \sigma_{w,ref}^2
\end{aligned} \quad (24)$$

The last expression shows a linear relation between the variance and the temporal-distance represented here in frame units,  $i$ . Translation of the temporal-distance to seconds (denoted as  $d_t$ ) is possible using (8):

$$\begin{aligned}
R_{e_i}(0, 0) = & 2(\sigma_{\Delta x}^2 + \sigma_{\Delta y}^2) \cdot \left[ \sigma_v^2 \cdot (1 - \rho_v) + \left( \frac{L}{F_{rate}} \tilde{\sigma}_q^2 + \sigma_{w,ref}^2 \right) \right] \\
& + 2\tilde{\sigma}_q^2 d_t + \sigma_{w,current}^2 + \sigma_{w,ref}^2
\end{aligned} \quad (25)$$

### 3.2 MC-Prediction of an Absent Frame

Let us consider temporal upsampling by a factor of  $D$  using MC-FRUC, i.e.,  $D - 1$  missing frames are interpolated between each two existing frames. The available frames are denoted as  $f_0$  and  $f_D$ , and the interpolated frames are denoted as  $\{\hat{f}_j\}_{j=1}^{D-1}$ . We consider the interpolation of a block in the  $j^{th}$  interpolated frame, where  $j \in \{1, \dots, D - 1\}$ . The corresponding unavailable frame is denoted as  $f_j$ .

The prediction includes estimation of the motion between the  $j^{th}$  frame and each of the available frames,  $f_0$  and  $f_D$ . The estimation is performed using  $f_0$  and  $f_D$ .  $\hat{\varphi}(j, 0 | f_0, f_D)$  and  $\hat{\varphi}(D, j | f_0, f_D)$  denote the estimated motion at  $f_j$  relative to frames  $f_0$  and  $f_D$ , respectively. We assume

$$\begin{aligned}
\hat{\varphi}(j, 0 | f_0, f_D) &= (\varphi_x(j, 0) + \Delta x_0^{abs}, \varphi_y(j, 0) + \Delta y_0^{abs}) \\
\hat{\varphi}(D, j | f_0, f_D) &= (\varphi_x(D, j) + \Delta x_D^{abs}, \varphi_y(D, j) + \Delta y_D^{abs})
\end{aligned} \quad (26)$$

Where  $\Delta x_0^{abs}$  and  $\Delta x_D^{abs}$  are assumed to be independent Gaussian random variables with zero-mean and variance

$$\sigma_{\Delta x^{abs}}^2 = \gamma_{abs} \cdot \sigma_{\Delta x}^2. \quad (27)$$

Where  $\sigma_{\Delta x}^2$  is the variance of  $\Delta x$ , which was defined above for the case of an available frame, and  $\gamma_{abs} > 1$  denotes effect of the frame absence on the spatial accuracy of the ME.  $\Delta y_0^{abs}$  and  $\Delta y_D^{abs}$  are defined accordingly by replacing  $x$  with  $y$ .

The overall prediction is calculated using two prediction signals. The backward prediction is defined as

$$\hat{f}_j(x, y | f_0, \hat{\varphi}(j, 0 | f_0, f_D)) = f_0(x - \hat{\varphi}_x(j, 0 | f_0, f_D), y - \hat{\varphi}_y(j, 0 | f_0, f_D)). \quad (28)$$

and the forward prediction as

$$\hat{f}_j(x, y | f_D, \hat{\varphi}(D, j | f_0, f_D)) = f_D(x + \hat{\varphi}_x(D, j | f_0, f_D), y + \hat{\varphi}_y(D, j | f_0, f_D)). \quad (29)$$

The final prediction is achieved by the following linear combination of (59) and (60):

$$\begin{aligned} \hat{f}_j^{final}(x, y | f_0, f_D) &= \theta \cdot \hat{f}_j(x, y | f_0, \hat{\varphi}(j, 0 | f_0, f_D)) \\ &\quad + [1 - \theta] \cdot \hat{f}_j(x, y | f_D, \hat{\varphi}(D, j | f_0, f_D)) \end{aligned} \quad (30)$$

and the prediction error is expressed as

$$e_{j|0,D}^{absent}(x, y) = f_j(x, y) - \hat{f}_j^{final}(x, y | f_0, f_D) \quad (31)$$

In appendix B, we describe in detail the calculation of the autocorrelation function of the MC-prediction error. This derivation results in

$$\begin{aligned} R_{e_{j|0,D}^{absent}}(k, l) &= \theta^2 \cdot R_{\Delta n_{j,0}}(k, l) + (1 - \theta)^2 \cdot R_{\Delta n_{D,j}}(k, l) + \\ &\quad + \sigma_{\Delta x^{abs}}^2 \cdot [\theta^2 + (1 - \theta)^2] \\ &\quad \times [2R_v(k, l) - R_v(k - 1, l) - R_v(k + 1, l) \\ &\quad \quad + 2R_{n_0}(k, l) - R_{n_0}(k - 1, l) - R_{n_0}(k + 1, l)] \\ &\quad + \sigma_{\Delta y^{abs}}^2 \cdot [\theta^2 + (1 - \theta)^2] \\ &\quad \times [2R_v(k, l) - R_v(k, l - 1) - R_v(k, l + 1) \\ &\quad \quad + 2R_{n_0}(k, l) - R_{n_0}(k, l - 1) - R_{n_0}(k, l + 1)] \end{aligned} \quad (32)$$

Let us study the variance of the error. This variance is also the mean-squared error (MSE) of the interpolation procedure; hence, it is useful for performance evaluation in applications such as FRUC. Using (4),(6) and (22), we calculate from (32) the following MSE expression.

$$\begin{aligned} R_{e_{j|0,D}^{absent}}(0, 0) &= \theta^2 \cdot [2\sigma_q^2 j + \sigma_{w_0}^2 + \sigma_{w_j}^2] \\ &\quad + (1 - \theta)^2 \cdot [2\sigma_q^2 (D - j) + \sigma_{w_0}^2 + \sigma_{w_j}^2] \\ &\quad + 2(\sigma_{\Delta x^{abs}}^2 + \sigma_{\Delta y^{abs}}^2) \cdot [\theta^2 + (1 - \theta)^2] \cdot [(1 - \rho_v) \cdot \sigma_v^2 + L\sigma_q^2 + \sigma_{w_0}^2] \end{aligned} \quad (33)$$

Usually,  $\theta$  is set to 0.5 for the central part of the interpolated block. We assume  $\theta = 0.5$  for the entire interpolated area; hence, (33) becomes

$$\begin{aligned} R_{e_{j|0,D}^{absent}}(0, 0) &= \frac{1}{2} \cdot [\sigma_q^2 D + \sigma_{w_0}^2 + \sigma_{w_j}^2] \\ &\quad + (\sigma_{\Delta x^{abs}}^2 + \sigma_{\Delta y^{abs}}^2) \cdot [(1 - \rho_v) \cdot \sigma_v^2 + L\sigma_q^2 + \sigma_{w_0}^2]. \end{aligned} \quad (34)$$

The last expression shows that the variance is a linear function of the temporal-distance between the available frames,  $D$ . Moreover, according to (8), the linear relation with  $\sigma_q^2$  implies a linear relation with the basic temporal-distance derived from the frame-rate. In addition, Recall that  $\sigma_{\Delta x^{abs}}^2$  and  $\sigma_{\Delta y^{abs}}^2$  are linear functions of  $D$  (27).

FRUC application may be applied on processed or reconstructed-from-compression video. The quality of the video affects FRUC performance. Our model supports these cases through the noise component of  $f_0$  and  $f_D$  frames; i.e., by including the processed video's MSE in  $\sigma_{w_0}^2$  and  $\sigma_{w_D}^2$ , as in (9) and (12).

## 4 A Simplified Autocorrelation Model for MC-Prediction Error in Coding

In section 3.1, we proposed an autocorrelation function for the error of MC-prediction of an available frame, as in coding applications. The proposed autocorrelation function (23) is rather complicated. Therefore, it may be useful to have also a simpler autocorrelation model. In this section, we propose a simpler autocorrelation model for the MC-residual in coding systems. The autocorrelation of MC-FRUC can be simplified similarly; however, it is unnecessary since FRUC analysis usually considers only the variance, which is equal to the interpolation MSE.

### 4.1 General Construction of A Separable Model

Similarly to [11] and [5], we construct a model of a separable form from the complicated autocorrelation function. As a result, the linearity of the variance in the temporal-distance is kept.

The variance-normalized autocorrelation function (ACF) is defined as

$$\rho_{e_i}(k, l) = \frac{R_{e_i}(k, l)}{R_{e_i}(0, 0)}. \quad (35)$$

The variance-normalized ACF along the horizontal axis is defined as

$$\rho_{e_i}^{horz}(k) = \frac{R_{e_i}(k, 0)}{R_{e_i}(0, 0)}. \quad (36)$$

The variance-normalized ACF along the vertical axis is defined correspondingly and denoted as  $\rho_{e_i}^{vert}(l)$ .

A separable form of  $R_{e_i}(k, l)$  is formed as follows:

$$R_{e_i}^{sep}(k, l) = R_{e_i}(0, 0) \cdot \rho_{e_i}^{horz}(k) \rho_{e_i}^{vert}(l) \quad (37)$$

Let us derive a separable model in the form of (37) for the autocorrelation function given in (23). This requires the calculation of  $R_{e_i}(0, 0)$ ,  $\rho_{e_i}^{horz}(k)$  and  $\rho_{e_i}^{vert}(l)$  that correspond to (24). The variance  $R_{e_i}(0, 0)$  is given in (24).

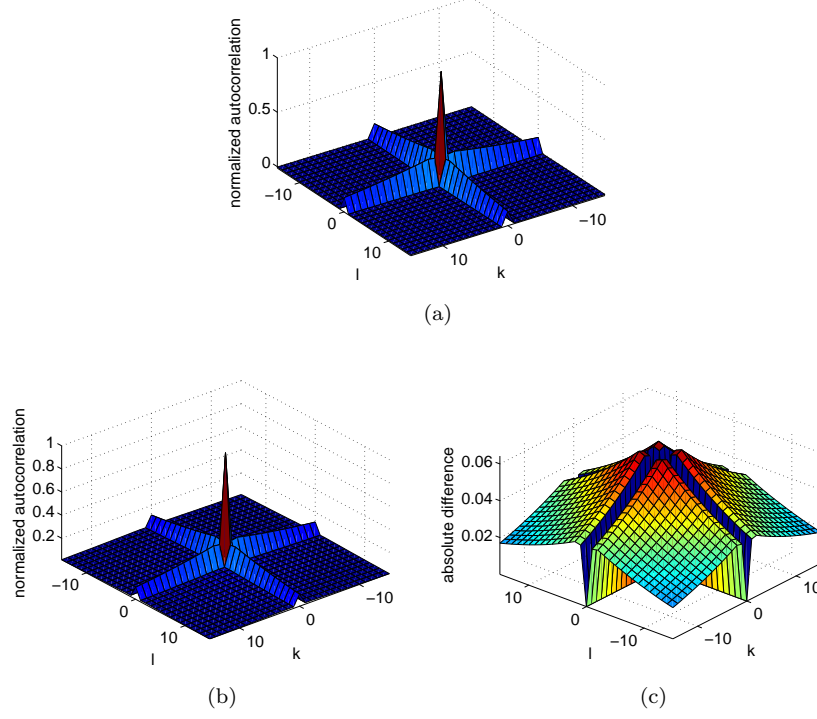


Figure 2: Estimation of MC-residual autocorrelation in MC-coding. (a) full model (23). (b) simplified model using separable construction (37). (c) absolute difference due to simplification.

First, we calculate  $R_{e_i}(k, 0)$  as follows.

$$\begin{aligned}
 R_{e_i}(k, 0) = & 2 \left[ \sigma_{\Delta x}^2 + \sigma_{\Delta y}^2 \right] \cdot \left[ \sigma_v^2 \cdot \rho_v^{|k|} + (L\sigma_q^2 + \sigma_{w,ref}^2) \cdot \delta(k) \right] \\
 & - \sigma_{\Delta x}^2 \sigma_v^2 \cdot \left[ \rho_v^{|k-1|} + \rho_v^{|k+1|} \right] \\
 & - \sigma_{\Delta x}^2 \cdot (L\sigma_q^2 + \sigma_{w,ref}^2) \cdot [\delta(k-1) + \delta(k+1)] \\
 & - 2\sigma_{\Delta y}^2 \sigma_v^2 \rho_v^{|k|+1} + (2i\sigma_q^2 + \sigma_{w,current}^2 + \sigma_{w,ref}^2) \cdot \delta(k)
 \end{aligned} \tag{38}$$

Then, we get  $\rho_{e_i}^{horz}(k)$  by dividing the last expression by  $R_{e_i}(0, 0)$  given in (24).  $\rho_{e_i}^{vert}(l)$  is achieved similarly by replacing  $x$  and  $k$  with  $y$  and  $l$ , respectively. Visual comparison of the original and simplified autocorrelation (Figs. 2a, 2b) shows high similarity while having acceptable differences (Fig. 2c).

## 4.2 A Separable First-Order Markov Model

While the autocorrelation function (23) was simplified to be separable (37), some users of the model may benefit from further simplification of the axis-ACF functions (e.g., (38)). We propose here to construct the autocorrelation

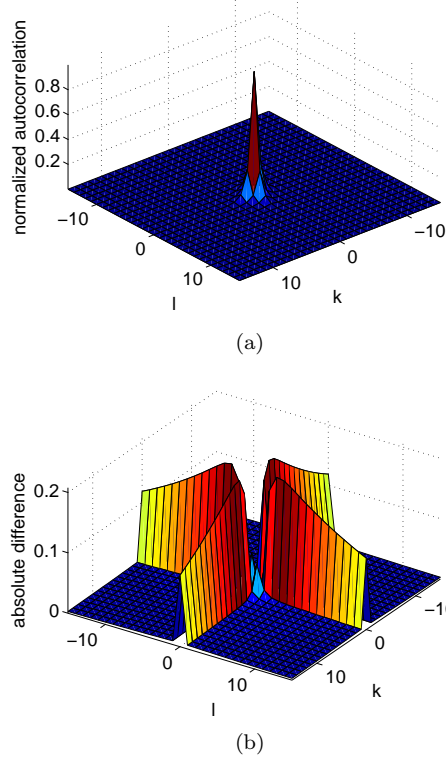


Figure 3: Simplified autocorrelation function using first-order Markov model. (a) normalized autocorrelation. (b) absolute difference from full model (23).

function as a separable first-order Markov model. As a result, the horizontal and vertical autocorrelation functions will be exponential, i.e.,

$$R_{e_i}^{Markov}(k, l) = R_{e_i}(0, 0) \cdot \rho_{h,e_i}^{|k|} \rho_{v,e_i}^{|l|}. \quad (39)$$

Where  $R_{e_i}$  and  $R_{e_i}(0, 0)$  are the autocorrelation and variance of the accurate model (23). We define the correlation coefficients as follows,

$$\rho_{h,e_i} = \frac{R_{e_i}(1, 0)}{R_{e_i}(0, 0)} \quad \text{and} \quad \rho_{v,e_i} = \frac{R_{e_i}(0, 1)}{R_{e_i}(0, 0)}. \quad (40)$$

This model differs from the accurate model (23) and the previous simplification (37) in its lower values along the horizontal and vertical axes (Fig. 3). However, for coordinates that are not on the main axes, the difference from the accurate model is small (Fig. 3b), even more than in the former simplified model (Fig. 2c). In general, we consider this Markov model as an acceptable estimation when its added simplicity is needed.

## 5 Theoretical Estimations

In this section we explore our model behavior for variation in main characteristics of the video signal and the compression procedure. We set  $\sigma_v^2 = 2312$ ,  $\rho_v = 0.95$  and  $L = 5$ . The local noise component,  $\sigma_w^2$ , was calculated as follows.  $\sigma_{w,basic}^2$  was set to zero, whereas  $\sigma_{w,compression}^2$  was calculated according to (10) with  $\alpha = 1$  and  $\beta = 10$ . We assume ME in half-pel accuracy; therefore,  $\Delta x, \Delta y \in [-0.25, 0.25]$  and  $\sigma_{\Delta x}^2 = \sigma_{\Delta y}^2 = (2 \times 0.25)^2 / 12$ .

### 5.1 Motion-Compensated Coding

First, we examine the estimated variance as the bit-rate varies (Fig. 4a). The variance is monotonically decreasing as the bit-rate increases, this is due to improved quality of the reference frame that increases its similarity to the coded frame. The graphs have a convex shape as expected from a distortion-rate function.

The estimated variance as the frame-rate varies is presented in (Fig. 4b). We assume the reference and the coded frames are adjacent, hence the frame-rate and the temporal-distance can be alternately referred using  $d_t = \frac{1}{F_{rate}}$ . The variance is linearly increasing as the temporal-distance increases. This is justified by the reduced similarity between the reference and coded frames as they get farther.

We compared our estimation for varying motion-complexity of the coded video expressed by  $\sigma_{q,basic}^2$  (Fig. 4c). The estimated variance increases together with the motion-complexity. This conforms with the fact that more complex motion affects the motion-estimation results and increases the MC-residual energy.

### 5.2 Motion-Compensated Frame-Rate Up Conversion

Let us consider our estimations for the MC-FRUC MSE (33), (34). The equations for the MC-FRUC MSE (34) and the residual variance in MC-coding (25) are similar; therefore, similar behavior is expected. The estimations (Fig. 5) conform with these expectations. The explanations given above for MC-coding (see section 5.1) also hold here.

## 6 Experimental Results

### 6.1 Motion-Compensated Coding

We measured the average MC-residual variance in an H.264 software [20] for the 'old town cross' and 'Parkrun' sequences (Fig. 6,7). The variance has a monotonically decreasing convex shape as function of the bit-rate (Figs. 6a, 7a), as in our model (Fig. 4a). In addition, the variance has a relatively linearly-increasing behavior as function of the temporal-distance (Figs. 6b, 7b), this

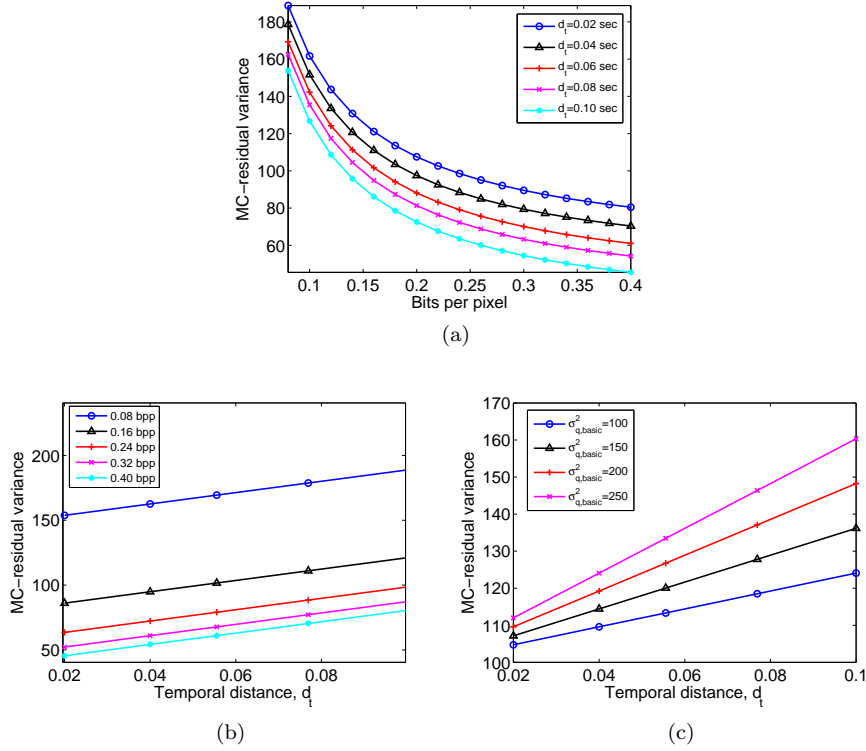


Figure 4: Estimation of MC-residual variance in MC-coding. (a) as function of bit-rate for various frame-rates (temporal distances). (b) as function of temporal-distance for various bit-rates. (c) as function of temporal-distance for various motion-energy values  $\sigma_{q,basic}^2$ .

also conforms with our model estimations (Fig. 4b). The 'parkrun' sequence contains more complex motion than 'old town cross'; as a result, its residual variance values are significantly higher (Figs. 6a, 7a). This is also expressed in our model (Fig. 4c).

## 6.2 Motion-Compensated Frame-Rate Up Conversion

In section 3.2 we gave an expression for the MC-FRUC error (34). Here we compare the behavior of the theoretical model with experimental results obtained from an MC-FRUC procedure implemented in Matlab. The variance of MC-prediction error in FRUC equals to the interpolation MSE; hence, we refer them here interchangeably. We examined the dependency of FRUC MSE in temporal-distance and bit-rate. For our experiments, we implemented an MC-FRUC algorithm that applies bidirectional motion-estimation with half-pel accuracy. We considered the central-interpolated frames for upsampling factors

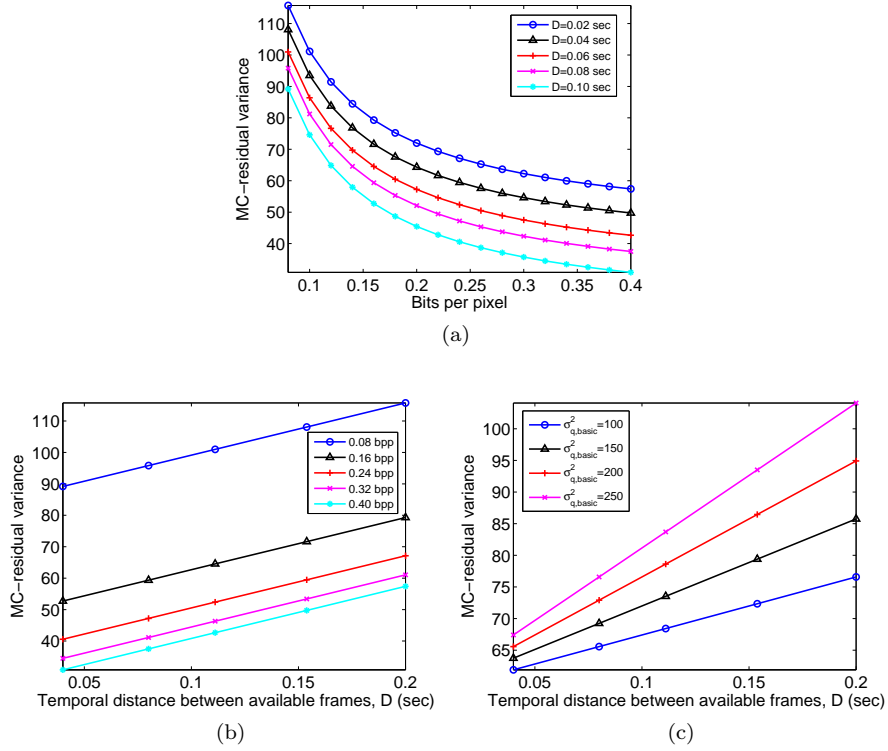
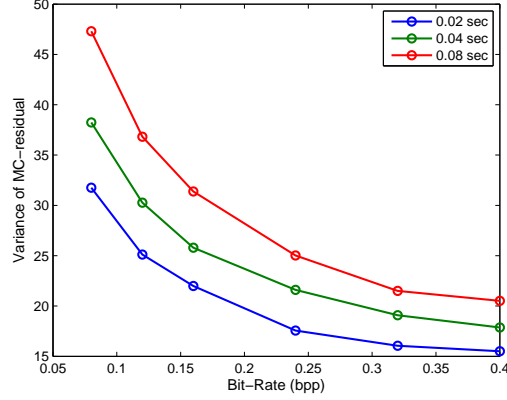


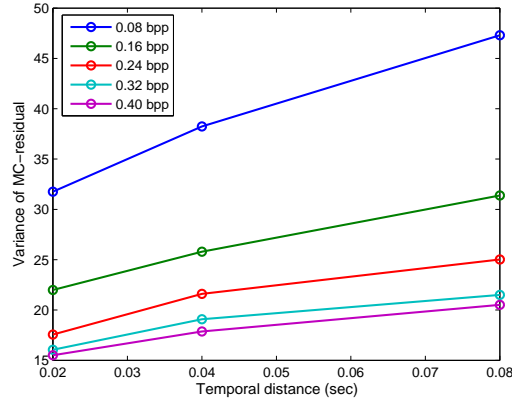
Figure 5: Estimation of MC-residual variance in MC-FRUC (i.e., estimation of interpolation MSE).  $\gamma_{abs} = 2$ . (a) as function of bit-rate for various interpolation factors (temporal distances). (b) as function of interpolation factors (temporal-distance) for various bit-rates. (c) as function of temporal-distance for various motion-energy values  $\sigma^2_{q,basic}$ .

$D = 2, 4, 6$  (i.e.,  $j = \frac{D}{2}$  for even  $D$  values). Hence, we studied the relation of the MSE to the temporal-distance by applying FRUC at a varying interpolation factor,  $D$ , for a fixed frame-rate. The experiments showed an approximately linear increment of the MSE together with the temporal-distance (Figs. 8b,9b,10b). In addition, its relation to the bit-rate has a convex-decreasing shape (Figs. 8a,9a,10a). 'Ice' sequence contains more static regions than 'Harbour', i.e., its motion is simpler. Accordingly, higher MSE values are observed for 'Harbour'. The above observations are expressed correspondingly in the theoretical estimations (Fig. 5).





(a)

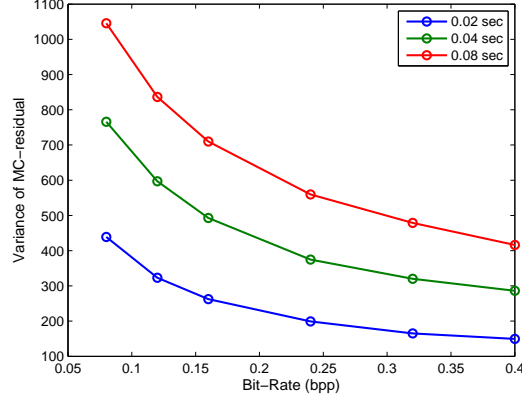


(b)

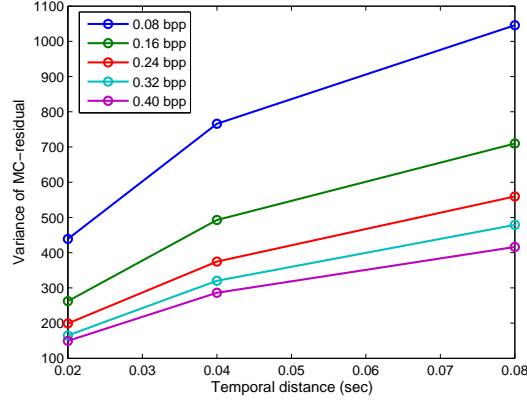
Figure 6: Measured MC-residual statistics in MC-coding of 'Old town cross' sequence (grayscale, frame size 720x720, 10 seconds length). (a) as function of bit-rate for various temporal-distance values. (b) as function of temporal-distance for various bit-rates.

## 7 Conclusion

The motion-compensation procedure was studied in this work. Both cases of predicting available and absent frames were theoretically examined, and expressions for the prediction error and its autocorrelation were given. The considered procedures represent the applications of MC in coding and FRUC. The analysis is based on a statistical model for the video signal that was presented in the beginning of this paper. Along this study, a special focus was given to the effects of frame-rate and bit-rate on the MC-prediction error. The MC applications in coding and FRUC were studied in the same theoretic framework. Hence, this



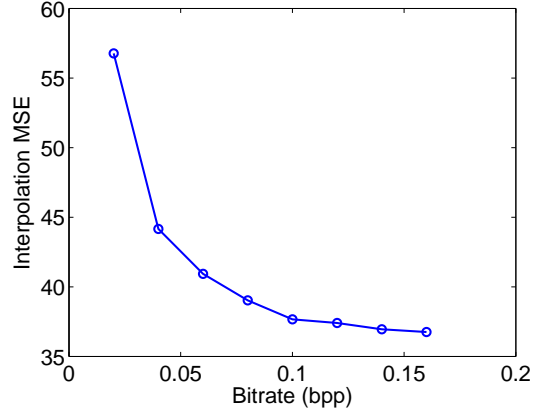
(a)



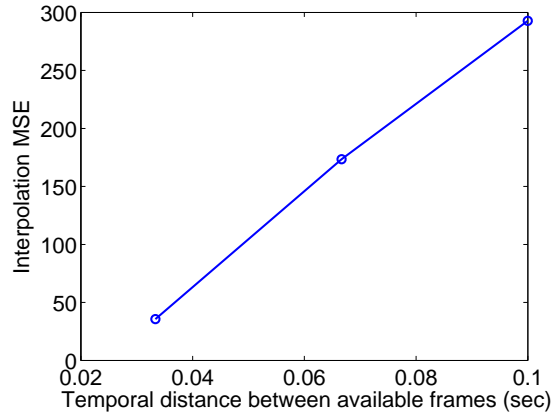
(b)

Figure 7: Measured MC-residual statistics in MC-coding of 'Parkrun' sequence (grayscale, frame size 720x720, 8 seconds length). (a) as function of bit-rate for various temporal-distance values. (b) as function of temporal-distance for various bit-rates.

paper can be seen as a comparison between the applications, as the similarities and differences raise from the text. For the application of MC-coding, we presented three autocorrelation models at different levels of analytic simplicity. Analytic simplicity is useful for examination of complex systems that include MC-coding. Future work can analyze such systems. This work emphasizes the significant effect of frame-rate and bit-rate on MC performance. Future work can suggest MC-related algorithms that consider these factors adaptively.

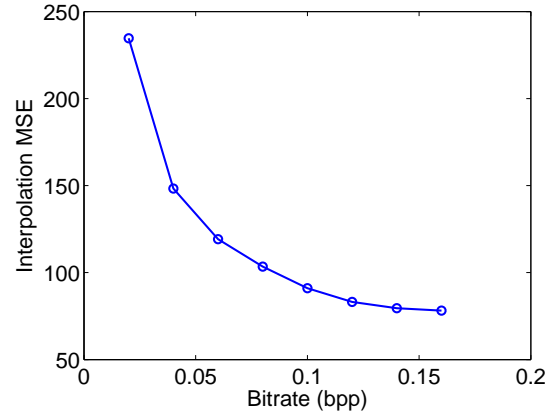


(a)

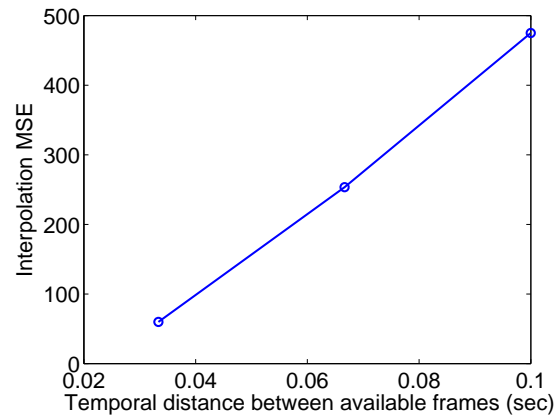


(b)

Figure 8: Measured MSE in MC-FRUC applied on 'Ice' sequence (grayscale, frame size 576x576, 60fps). (a) as function of bit-rate. (b) as function of temporal-distance (i.e., varying temporal-interpolation factors) for raw video.

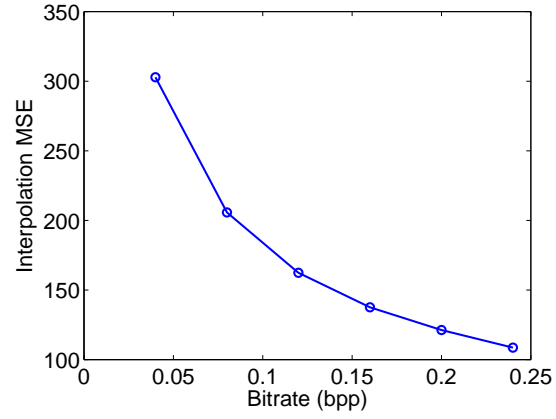


(a)

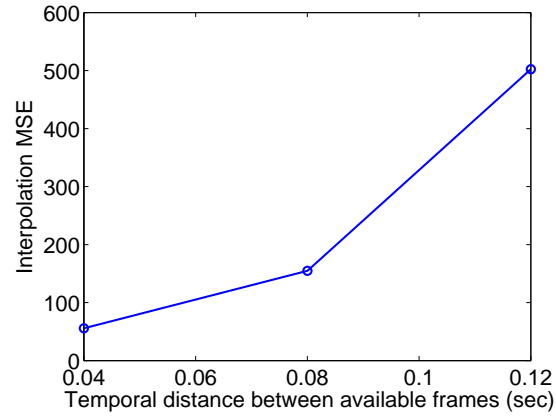


(b)

Figure 9: Measured MSE in MC-FRUC applied on 'Harbour' sequence (grayscale, frame size 576x576, 60fps). (a) as function of bit-rate. (b) as function of temporal-distance (i.e., varying temporal-interpolation factors) for raw video.



(a)



(b)

Figure 10: Measured MSE in MC-FRUC applied on 'Parkrun' sequence (grayscale, frame size 720x720, 50fps). (a) as function of bit-rate. (b) as function of temporal-distance (i.e., varying temporal-interpolation factors) for raw video.

## A Autocorrelation Calculation for Prediction of an Available Frame

Here we calculate the autocorrelation of the MC-prediction residual for the case of an available frame that was presented in section 3.1. Recall the expression given in (18) for the MC-prediction:

$$\begin{aligned} \hat{f}_t \left( x, y \left| f_{t-i}^{ref}, \hat{\varphi}(t, t-i | f_t, f_{t-i}) \right. \right) &= v(x - \varphi_x(t, 0) - \Delta x, y - \varphi_y(t, 0) - \Delta y) \\ &+ n_{t-i}^{ref}(x - \hat{\varphi}_x(t, t-i | f_t, f_{t-i}), y - \hat{\varphi}_y(t, t-i | f_t, f_{t-i})) \end{aligned} \quad (41)$$

Let us assume that  $\Delta x$  and  $\Delta y$  are small. Then, first-order Taylor expansion gives the following approximations

$$\begin{aligned} v(x - \varphi_x(t, 0) - \Delta x, y - \varphi_y(t, 0) - \Delta y) &\approx v(x - \varphi_x(t, 0), y - \varphi_y(t, 0)) \\ &- \Delta x \frac{\partial}{\partial \tilde{x}} v(\tilde{x}, \tilde{y}) \Big|_{(\tilde{x}, \tilde{y})=(x-\varphi_x(t,0), y-\varphi_y(t,0))} \\ &- \Delta y \frac{\partial}{\partial \tilde{y}} v(\tilde{x}, \tilde{y}) \Big|_{(\tilde{x}, \tilde{y})=(x-\varphi_x(t,0), y-\varphi_y(t,0))} \end{aligned} \quad (42)$$

$$\begin{aligned} n_{t-i}(x - \hat{\varphi}_x(t, t-i | f_t, f_{t-i}), y - \hat{\varphi}_y(t, t-i | f_t, f_{t-i})) &\approx \\ n_{t-i}(x - \varphi_x(t, t-i), y - \varphi_y(t, t-i)) \\ &- \Delta x \frac{\partial}{\partial \tilde{x}} n_{t-i}(\tilde{x}, \tilde{y}) \Big|_{(\tilde{x}, \tilde{y})=(x-\varphi_x(t,t-i), y-\varphi_y(t,t-i))} \\ &- \Delta y \frac{\partial}{\partial \tilde{y}} n_{t-i}(\tilde{x}, \tilde{y}) \Big|_{(\tilde{x}, \tilde{y})=(x-\varphi_x(t,t-i), y-\varphi_y(t,t-i))} \end{aligned} \quad (43)$$

Substitution of (42) and (43) into (18) yields

$$\begin{aligned} \hat{f}_t \left( x, y \left| f_{t-i}^{ref}, \hat{\varphi}(t, t-i | f_t, f_{t-i}) \right. \right) &= v(x - \varphi_x(t, 0), y - \varphi_y(t, 0)) \\ &+ n_{t-i}^{ref}(x - \varphi_x(t, t-i), y - \varphi_y(t, t-i)) \\ &- \Delta x \frac{\partial}{\partial \tilde{x}} v(\tilde{x}, \tilde{y}) \Big|_{(\tilde{x}, \tilde{y})=(x-\varphi_x(t,0), y-\varphi_y(t,0))} \\ &- \Delta y \frac{\partial}{\partial \tilde{y}} v(\tilde{x}, \tilde{y}) \Big|_{(\tilde{x}, \tilde{y})=(x-\varphi_x(t,0), y-\varphi_y(t,0))} \\ &- \Delta x \frac{\partial}{\partial \tilde{x}} n_{t-i}^{ref}(\tilde{x}, \tilde{y}) \Big|_{(\tilde{x}, \tilde{y})=(x-\varphi_x(t,t-i), y-\varphi_y(t,t-i))} \\ &- \Delta y \frac{\partial}{\partial \tilde{y}} n_{t-i}^{ref}(\tilde{x}, \tilde{y}) \Big|_{(\tilde{x}, \tilde{y})=(x-\varphi_x(t,t-i), y-\varphi_y(t,t-i))} \end{aligned} \quad (44)$$

The MC-prediction error of  $f_t$  using  $f_{t-i}$  as a reference frame was formulated in (19) as

$$e_{t|t-i}(x, y) = f_t(x, y) - \hat{f}_t \left( x, y \left| f_{t-i}^{ref}, \hat{\varphi}(t, t-i | f_t, f_{t-i}) \right. \right) \quad (45)$$

Setting (7) and (44) into (45) yields

$$\begin{aligned}
e_{t|t-i}(x, y) = & \Delta x \frac{\partial}{\partial \tilde{x}} v(\tilde{x}, \tilde{y}) \Big|_{(\tilde{x}, \tilde{y})=(x-\varphi_x(t,0), y-\varphi_y(t,0))} \\
& + \Delta y \frac{\partial}{\partial \tilde{y}} v(\tilde{x}, \tilde{y}) \Big|_{(\tilde{x}, \tilde{y})=(x-\varphi_x(t,0), y-\varphi_y(t,0))} \\
& + \Delta x \frac{\partial}{\partial \tilde{x}} n_{t-i}^{ref}(\tilde{x}, \tilde{y}) \Big|_{(\tilde{x}, \tilde{y})=(x-\varphi_x(t,t-i), y-\varphi_y(t,t-i))} \\
& + \Delta y \frac{\partial}{\partial \tilde{y}} n_{t-i}^{ref}(\tilde{x}, \tilde{y}) \Big|_{(\tilde{x}, \tilde{y})=(x-\varphi_x(t,t-i), y-\varphi_y(t,t-i))} \\
& + n_t(x, y) \\
& - n_{t-i}^{ref}(x - \varphi_x(t, t-i), y - \varphi_y(t, t-i))
\end{aligned} \tag{46}$$

We simplify the last expression by defining the motion-compensated noise difference, denoted as  $\Delta n_{t_2, t_1}$  for  $t_1 < t_2$ :

$$\Delta n_{t_2, t_1}(x, y) \equiv n_{t_2}(x, y) - n_{t_1}^{ref}(x - \varphi_x(t_2, t_1), y - \varphi_y(t_2, t_1)) \tag{47}$$

Let us calculate  $\Delta n_{t_2, t_1}$  for  $t_2 - t_1 \leq L$ . Using  $n_t$ 's definition in (5), and the corresponding  $n_t^{ref}$  definition, we get

$$\begin{aligned}
\Delta n_{t_2, t_1}(x, y) = & w_{t_2}(x, y) + \sum_{j=t_2-L+1}^{t_2} q_j(x - \varphi_x(t_2, j), y - \varphi_y(t_2, j)) \\
& - w_{t_1}^{ref}(x - \varphi_x(t_2, t_1), y - \varphi_y(t_2, t_1)) \\
& - \sum_{h=t_1-L+1}^{t_1} q_h(x - \varphi_x(t_2, t_1) - \varphi_x(t_1, h), y - \varphi_y(t_2, t_1) - \varphi_y(t_1, h)) \\
= & w_{t_2}(x, y) - w_{t_1}^{ref}(x - \varphi_x(t_2, t_1), y - \varphi_y(t_2, t_1)) \\
& + \sum_{j=t_1+1}^{t_2} q_j(x - \varphi_x(t_2, j), y - \varphi_y(t_2, j)) \\
& - \sum_{h=t_1-L+1}^{t_2-L} q_h(x - \varphi_x(t_2, h), y - \varphi_y(t_2, h))
\end{aligned} \tag{48}$$

From  $q_t$  and  $w_t$ 's independence property we get

$$\begin{aligned}
R_{\Delta n_{t_2, t_1}}(k, l) = & \left[ 2\sigma_q^2 \cdot (t_2 - t_1) + \sigma_{w_{t_1}}^2 + \sigma_{w_{t_2}}^2 \right] \cdot \delta(k, l) \\
= & \left[ 2\sigma_q^2 \cdot (t_2 - t_1) + 2\sigma_{w, basic}^2 + \sigma_{w, compression}^2 \right] \cdot \delta(k, l)
\end{aligned} \tag{49}$$

Let us calculate the autocorrelation of the error

$$R_{e_i}(k, l) = E \{ e_{t|t-i}(x, y) \cdot e_{t|t-i}(x + k, y + l) \} \tag{50}$$

In order to calculate  $R_{e_i}$ , we first analyze relations among the elements in  $e_{t|t-i}$ 's expression (46). Recall that  $\Delta x$  and  $\Delta y$  are zero-mean independent variables;

hence,  $E\{\Delta x \Delta y\} = 0$ . Moreover,  $\Delta x$  and  $\Delta y$  are independent with  $v$  and  $n_j$  for any  $j$ ; therefore, they are also independent with derivatives of  $v$  and  $n_j$ , and the following relations hold

$$\begin{aligned}
E\left\{\left(\Delta x \frac{\partial}{\partial \tilde{x}} v(\tilde{x}, \tilde{y})\right)^2\right\} &= E\{\Delta x^2\} \cdot E\left\{\left(\frac{\partial}{\partial \tilde{x}} v(\tilde{x}, \tilde{y})\right)^2\right\} \\
E\left\{\left(\Delta x \frac{\partial}{\partial \tilde{x}} n_j(\tilde{x}, \tilde{y})\right)^2\right\} &= E\{\Delta x^2\} \cdot E\left\{\left(\frac{\partial}{\partial \tilde{x}} n_j(\tilde{x}, \tilde{y})\right)^2\right\} \\
E\left\{\Delta x \cdot \frac{\partial}{\partial \tilde{x}} v(\tilde{x}, \tilde{y}) \cdot \Delta n_{t,t-i}(x, y)\right\} &= E\{\Delta x\} \cdot E\left\{\frac{\partial}{\partial \tilde{x}} v(\tilde{x}, \tilde{y})\right\} \cdot E\{\Delta n_{t,t-i}(x, y)\} = 0 \\
E\left\{\Delta x \cdot \frac{\partial}{\partial \tilde{x}} n_{t-i}(\tilde{x}, \tilde{y}) \cdot \Delta n_{t,t-i}(x, y)\right\} &= E\{\Delta x\} \cdot E\left\{\frac{\partial}{\partial \tilde{x}} n_{t-i}(\tilde{x}, \tilde{y})\right\} \cdot E\{\Delta n_{t,t-i}(x, y)\} = 0
\end{aligned} \tag{51}$$

$n_j(x, y)$  is zero-mean and independent with  $v(x, y)$ , we utilize this in the following calculation.

$$\begin{aligned}
E\left\{\frac{\partial}{\partial \tilde{x}} v(\tilde{x}, \tilde{y}) \cdot \frac{\partial}{\partial \tilde{x}} n_j(\tilde{x}, \tilde{y})\right\} \\
\approx E\left\{\left(\frac{v(\tilde{x} + \varepsilon_v, \tilde{y}) - v(\tilde{x}, \tilde{y})}{\varepsilon_v}\right) \cdot \left(\frac{n_j(\tilde{x} + \varepsilon_n, \tilde{y}) - n_j(\tilde{x}, \tilde{y})}{\varepsilon_n}\right)\right\} \\
= E\left\{\frac{v(\tilde{x} + \varepsilon_v, \tilde{y}) - v(\tilde{x}, \tilde{y})}{\varepsilon_v}\right\} \cdot E\left\{\frac{n_j(\tilde{x} + \varepsilon_n, \tilde{y}) - n_j(\tilde{x}, \tilde{y})}{\varepsilon_n}\right\} \\
= E\left\{\frac{v(\tilde{x} + \varepsilon_v, \tilde{y}) - v(\tilde{x}, \tilde{y})}{\varepsilon_v}\right\} \cdot 0 = 0
\end{aligned} \tag{52}$$

Where  $\varepsilon_v$  and  $\varepsilon_n$  are very small. (51)-(52) hold for  $y$  by replacing  $x$  with  $y$ .

Let us return to  $R_{e_i}$ 's calculation started in (50). We define  $\sigma_{\Delta x}^2 \equiv E\{\Delta x^2\}$  and  $\sigma_{\Delta y}^2 \equiv E\{\Delta y^2\}$ . Additionally, we define the following notation for the autocorrelation of the derivative of a function  $f$ :

$$\begin{aligned}
autocorr\left\{\frac{\partial}{\partial \tilde{x}} f(\tilde{x}, \tilde{y})\right\}_{(\tilde{x}, \tilde{y})=(x, y)}(k, l) &\equiv \\
E\left\{\frac{\partial}{\partial \tilde{x}} f(\tilde{x}, \tilde{y})\right\}_{(\tilde{x}, \tilde{y})=(x, y)} \cdot \frac{\partial}{\partial \tilde{x}} f(\tilde{x}, \tilde{y})\Big|_{(\tilde{x}, \tilde{y})=(x+k, y+l)}\right\}
\end{aligned} \tag{53}$$

We use (51)-(53) to get

$$\begin{aligned}
R_{e_i}(k, l) &= \sigma_{\Delta x}^2 \cdot autocorr\left\{\frac{\partial}{\partial \tilde{x}} v(\tilde{x}, \tilde{y})\right\}_{(\tilde{x}, \tilde{y})=(\tilde{x}_0, \tilde{y}_0)}(k, l) \\
&\quad + \sigma_{\Delta y}^2 \cdot autocorr\left\{\frac{\partial}{\partial \tilde{y}} v(\tilde{x}, \tilde{y})\right\}_{(\tilde{x}, \tilde{y})=(\tilde{x}_0, \tilde{y}_0)}(k, l) \\
&\quad + \sigma_{\Delta x}^2 \cdot autocorr\left\{\frac{\partial}{\partial \tilde{x}} n_{t-i}^{ref}(\tilde{x}, \tilde{y})\right\}_{(\tilde{x}, \tilde{y})=(\tilde{x}_i, \tilde{y}_i)}(k, l)
\end{aligned} \tag{54}$$



$$\begin{aligned}
& + \sigma_{\Delta y}^2 \cdot autocorr \left\{ \frac{\partial}{\partial \tilde{y}} n_{t-i}^{ref}(\tilde{x}, \tilde{y}) \Big|_{(\tilde{x}, \tilde{y})=(\tilde{x}_i, \tilde{y}_i)} \right\} (k, l) \\
& + E \{ \Delta n_{t, t-i}(x, y) \cdot \Delta n_{t, t-i}(x+k, y+l) \}
\end{aligned}$$

where  $(\tilde{x}_0, \tilde{y}_0) = (x - \varphi_x(t, 0), y - \varphi_y(t, 0))$  and  $(\tilde{x}_i, \tilde{y}_i) = (x - \varphi_x(t, t-i), y - \varphi_y(t, t-i))$ .

The discrete derivative approximation is

$$\frac{\partial}{\partial \tilde{x}} f(\tilde{x}, \tilde{y}) \Big|_{(\tilde{x}, \tilde{y})=(x, y)} \approx f(x+1, y) - f(x, y). \quad (55)$$

By using this approximation, we represent the derivative autocorrelation as function of  $f$ 's autocorrelation,  $R_f$ :

$$\begin{aligned}
& autocorr \left\{ \frac{\partial}{\partial \tilde{x}} f(\tilde{x}, \tilde{y}) \Big|_{(\tilde{x}, \tilde{y})=(x, y)} \right\} (k, l) \\
& = E \{ [f(x+1, y) - f(x, y)] \cdot [f(x+1+k, y+l) - f(x+k, y+l)] \} \\
& = 2R_f(k, l) - R_f(k-1, l) - R_f(k+1, l)
\end{aligned} \quad (56)$$

We use (56) to eliminate the derivative operators in (54):

$$\begin{aligned}
R_{e_i}(k, l) = & 2 [\sigma_{\Delta x}^2 + \sigma_{\Delta y}^2] \cdot [R_v(k, l) + R_{n_{t-i}^{ref}}(k, l)] \\
& - \sigma_{\Delta x}^2 \cdot [R_v(k-1, l) + R_v(k+1, l)] \\
& - \sigma_{\Delta x}^2 \cdot [R_{n_{t-i}^{ref}}(k-1, l) + R_{n_{t-i}^{ref}}(k+1, l)] \\
& - \sigma_{\Delta y}^2 \cdot [R_v(k, l-1) + R_v(k, l+1)] \\
& - \sigma_{\Delta y}^2 \cdot [R_{n_{t-i}^{ref}}(k, l-1) + R_{n_{t-i}^{ref}}(k, l+1)] \\
& + R_{\Delta n_{t, t-i}}(k, l)
\end{aligned} \quad (57)$$

Substituting autocorrelation expressions from (4), (6) and (49) into (57) yields

$$\begin{aligned}
R_{e_i}(k, l) = & 2 [\sigma_{\Delta x}^2 + \sigma_{\Delta y}^2] \cdot \left[ \sigma_v^2 \cdot \rho_v^{|k|+|l|} + (L\sigma_q^2 + \sigma_{w,ref}^2) \cdot \delta(k, l) \right] \\
& - \sigma_{\Delta x}^2 \sigma_v^2 \rho_v^{|l|} \cdot [\rho_v^{|k-1|} + \rho_v^{|k+1|}] \\
& - \sigma_{\Delta x}^2 [L\sigma_q^2 + \sigma_{w,ref}^2] \cdot [\delta(k-1, l) + \delta(k+1, l)] \\
& - \sigma_{\Delta y}^2 \sigma_v^2 \rho_v^{|k|} \cdot [\rho_v^{|l-1|} + \rho_v^{|l+1|}] \\
& - \sigma_{\Delta y}^2 [L\sigma_q^2 + \sigma_{w,ref}^2] \cdot [\delta(k, l-1) + \delta(k, l+1)] \\
& + [2i\sigma_q^2 + \sigma_{w,current}^2 + \sigma_{w,ref}^2] \cdot \delta(k, l)
\end{aligned} \quad (58)$$

## B Autocorrelation Calculation for Prediction of an Absent Frame

Here we calculate the autocorrelation of the MC-prediction residual for the case of an available frame that was presented in section 3.2. Recall our definitions from section 3.2 for the backward prediction:

$$\hat{f}_j(x, y | f_0, \hat{\varphi}(j, 0 | f_0, f_D)) = f_0(x - \hat{\varphi}_x(j, 0 | f_0, f_D), y - \hat{\varphi}_y(j, 0 | f_0, f_D)). \quad (59)$$

and the forward prediction:

$$\hat{f}_j(x, y | f_D, \hat{\varphi}(D, j | f_0, f_D)) = f_D(x + \hat{\varphi}_x(D, j | f_0, f_D), y + \hat{\varphi}_y(D, j | f_0, f_D)). \quad (60)$$

Similar to (44), we get

$$\begin{aligned} \hat{f}_j(x, y | f_0, \hat{\varphi}(j, 0 | f_0, f_D)) &= v(x - \varphi_x(j, 0), y - \varphi_y(j, 0)) \\ &\quad - \Delta x_0^{abs} \frac{\partial}{\partial \tilde{x}} v(\tilde{x}, \tilde{y}) \Big|_{(\tilde{x}, \tilde{y})=(x-\varphi_x(j,0), y-\varphi_y(j,0))} \\ &\quad - \Delta y_0^{abs} \frac{\partial}{\partial \tilde{y}} v(\tilde{x}, \tilde{y}) \Big|_{(\tilde{x}, \tilde{y})=(x-\varphi_x(j,0), y-\varphi_y(j,0))} \\ &\quad + n_0(x - \varphi_x(j, 0), y - \varphi_y(j, 0)) \\ &\quad - \Delta x_0^{abs} \frac{\partial}{\partial \tilde{x}} n_0(\tilde{x}, \tilde{y}) \Big|_{(\tilde{x}, \tilde{y})=(x-\varphi_x(j,0), y-\varphi_y(j,0))} \\ &\quad - \Delta y_0^{abs} \frac{\partial}{\partial \tilde{y}} n_0(\tilde{x}, \tilde{y}) \Big|_{(\tilde{x}, \tilde{y})=(x-\varphi_x(j,0), y-\varphi_y(j,0))} \end{aligned} \quad (61)$$

and

$$\begin{aligned} \hat{f}_j(x, y | f_D, \hat{\varphi}(D, j | f_0, f_D)) &= v(x - \varphi_x(j, 0), y - \varphi_y(j, 0)) \\ &\quad + \Delta x_D^{abs} \frac{\partial}{\partial \tilde{x}} v(\tilde{x}, \tilde{y}) \Big|_{(\tilde{x}, \tilde{y})=(x-\varphi_x(j,0), y-\varphi_y(j,0))} \\ &\quad + \Delta y_D^{abs} \frac{\partial}{\partial \tilde{y}} v(\tilde{x}, \tilde{y}) \Big|_{(\tilde{x}, \tilde{y})=(x-\varphi_x(j,0), y-\varphi_y(j,0))} \\ &\quad + n_D(x + \varphi_x(D, j), y + \varphi_y(D, j)) \\ &\quad + \Delta x_D^{abs} \frac{\partial}{\partial \tilde{x}} n_D(\tilde{x}, \tilde{y}) \Big|_{(\tilde{x}, \tilde{y})=(x+\varphi_x(D,j), y+\varphi_y(D,j))} \\ &\quad + \Delta y_D^{abs} \frac{\partial}{\partial \tilde{y}} n_D(\tilde{x}, \tilde{y}) \Big|_{(\tilde{x}, \tilde{y})=(x+\varphi_x(D,j), y+\varphi_y(D,j))} \end{aligned} \quad (62)$$

The final prediction was defined in (30) as

$$\begin{aligned} \hat{f}_j^{final}(x, y | f_0, f_D) &= \theta \cdot \hat{f}_j(x, y | f_0, \hat{\varphi}(j, 0 | f_0, f_D)) \\ &\quad + [1 - \theta] \cdot \hat{f}_j(x, y | f_D, \hat{\varphi}(D, j | f_0, f_D)) \end{aligned} \quad (63)$$

Setting (61) and (62) into (63) yields

$$\begin{aligned}
\hat{f}_j^{final}(x, y | f_0, f_D) = & v(x - \varphi_x(j, 0), y - \varphi_y(j, 0)) \\
& - [\theta \cdot \Delta x_0^{abs} - (1 - \theta) \cdot \Delta x_D^{abs}] \cdot \frac{\partial}{\partial \tilde{x}} v(\tilde{x}, \tilde{y}) \Big|_{(\tilde{x}, \tilde{y})=(x-\varphi_x(j,0), y-\varphi_y(j,0))} \\
& - [\theta \cdot \Delta y_0^{abs} - (1 - \theta) \cdot \Delta y_D^{abs}] \cdot \frac{\partial}{\partial \tilde{y}} v(\tilde{x}, \tilde{y}) \Big|_{(\tilde{x}, \tilde{y})=(x-\varphi_x(j,0), y-\varphi_y(j,0))} \\
& + \theta \cdot \left[ n_0(x - \varphi_x(j, 0), y - \varphi_y(j, 0)) \right. \\
& \quad - \Delta x_0^{abs} \frac{\partial}{\partial \tilde{x}} n_0(\tilde{x}, \tilde{y}) \Big|_{(\tilde{x}, \tilde{y})=(x-\varphi_x(j,0), y-\varphi_y(j,0))} \\
& \quad \left. - \Delta y_0^{abs} \frac{\partial}{\partial \tilde{y}} n_0(\tilde{x}, \tilde{y}) \Big|_{(\tilde{x}, \tilde{y})=(x-\varphi_x(j,0), y-\varphi_y(j,0))} \right] \\
& + (1 - \theta) \cdot \left[ n_D(x + \varphi_x(D, j), y + \varphi_y(D, j)) \right. \\
& \quad + \Delta x_D^{abs} \frac{\partial}{\partial \tilde{x}} n_D(\tilde{x}, \tilde{y}) \Big|_{(\tilde{x}, \tilde{y})=(x+\varphi_x(D,j), y+\varphi_y(D,j))} \\
& \quad \left. + \Delta y_D^{abs} \frac{\partial}{\partial \tilde{y}} n_D(\tilde{x}, \tilde{y}) \Big|_{(\tilde{x}, \tilde{y})=(x+\varphi_x(D,j), y+\varphi_y(D,j))} \right]
\end{aligned} \tag{64}$$

The prediction error was defined in (68) as

$$e_{j|0,D}^{absent}(x, y) = f_j(x, y) - \hat{f}_j^{final}(x, y | f_0, f_D) \tag{65}$$

We develop the last error expression as follows:

$$\begin{aligned}
e_{j|0,D}^{absent}(x, y) = & f_j(x, y) - \hat{f}_j^{final}(x, y | f_0, f_D) \\
= & n_j(x, y) + [\theta \Delta x_0^{abs} - (1 - \theta) \Delta x_D^{abs}] \cdot \frac{\partial}{\partial \tilde{x}} v(\tilde{x}, \tilde{y}) \Big|_{(\tilde{x}, \tilde{y})=(x-\varphi_x(j,0), y-\varphi_y(j,0))} \\
& + [\theta \Delta y_0^{abs} - (1 - \theta) \Delta y_D^{abs}] \cdot \frac{\partial}{\partial \tilde{y}} v(\tilde{x}, \tilde{y}) \Big|_{(\tilde{x}, \tilde{y})=(x-\varphi_x(j,0), y-\varphi_y(j,0))} \\
& - \theta \left[ n_0(x - \varphi_x(j, 0), y - \varphi_y(j, 0)) \right. \\
& \quad - \Delta x_0^{abs} \frac{\partial}{\partial \tilde{x}} n_0(\tilde{x}, \tilde{y}) \Big|_{(\tilde{x}, \tilde{y})=(x-\varphi_x(j,0), y-\varphi_y(j,0))} \\
& \quad \left. - \Delta y_0^{abs} \frac{\partial}{\partial \tilde{y}} n_0(\tilde{x}, \tilde{y}) \Big|_{(\tilde{x}, \tilde{y})=(x-\varphi_x(j,0), y-\varphi_y(j,0))} \right] \\
& - (1 - \theta) \left[ n_D(x + \varphi_x(D, j), y + \varphi_y(D, j)) \right.
\end{aligned} \tag{66}$$

$$\begin{aligned}
& + \Delta x_D^{abs} \frac{\partial}{\partial \tilde{x}} n_D(\tilde{x}, \tilde{y}) \Big|_{(\tilde{x}, \tilde{y})=(x+\varphi_x(D,j), y+\varphi_y(D,j))} \\
& + \Delta y_D^{abs} \frac{\partial}{\partial \tilde{y}} n_D(\tilde{x}, \tilde{y}) \Big|_{(\tilde{x}, \tilde{y})=(x+\varphi_x(D,j), y+\varphi_y(D,j))} \Big] \\
& = \theta [n_j(x, y) - n_0(x - \varphi_x(j, 0), y - \varphi_y(j, 0))] \\
& \quad - (1 - \theta) [n_D(x + \varphi_x(D, j), y + \varphi_y(D, j)) - n_j(x, y)] \\
& \quad + [\theta \Delta x_0^{abs} - (1 - \theta) \Delta x_D^{abs}] \cdot \frac{\partial}{\partial \tilde{x}} v(\tilde{x}, \tilde{y}) \Big|_{(\tilde{x}, \tilde{y})=(x-\varphi_x(j,0), y-\varphi_y(j,0))} \\
& \quad + [\theta \Delta y_0^{abs} - (1 - \theta) \Delta y_D^{abs}] \cdot \frac{\partial}{\partial \tilde{y}} v(\tilde{x}, \tilde{y}) \Big|_{(\tilde{x}, \tilde{y})=(x-\varphi_x(j,0), y-\varphi_y(j,0))} \\
& \quad + \theta \left[ \Delta x_0^{abs} \frac{\partial}{\partial \tilde{x}} n_0(\tilde{x}, \tilde{y}) \Big|_{(\tilde{x}, \tilde{y})=(x-\varphi_x(j,0), y-\varphi_y(j,0))} \right. \\
& \quad \quad \left. + \Delta y_0^{abs} \frac{\partial}{\partial \tilde{y}} n_0(\tilde{x}, \tilde{y}) \Big|_{(\tilde{x}, \tilde{y})=(x-\varphi_x(j,0), y-\varphi_y(j,0))} \right] \\
& \quad - (1 - \theta) \left[ \Delta x_D^{abs} \frac{\partial}{\partial \tilde{x}} n_D(\tilde{x}, \tilde{y}) \Big|_{(\tilde{x}, \tilde{y})=(x+\varphi_x(D,j), y+\varphi_y(D,j))} \right. \\
& \quad \quad \left. + \Delta y_D^{abs} \frac{\partial}{\partial \tilde{y}} n_D(\tilde{x}, \tilde{y}) \Big|_{(\tilde{x}, \tilde{y})=(x+\varphi_x(D,j), y+\varphi_y(D,j))} \right]
\end{aligned}$$

From  $\Delta n$ 's definition in (21) we get

$$\Delta n_{j,0}(x, y) = n_j(x, y) - n_0(x - \varphi_x(j, 0), y - \varphi_y(j, 0)) \quad (67)$$

$$\Delta n_{D,j}(x + \varphi_x(D, j), y + \varphi_y(D, j)) = n_D(x + \varphi_x(D, j), y + \varphi_y(D, j)) - n_j(x, y)$$

Inserting (67) into (66) yields

$$\begin{aligned}
e_{j|0,D}^{absent}(x, y) & = \theta \cdot \Delta n_{j,0}(x, y) \quad (68) \\
& \quad - (1 - \theta) \cdot \Delta n_{D,j}(x + \varphi_x(D, j), y + \varphi_y(D, j)) \\
& \quad + [\theta \cdot \Delta x_0^{abs} - (1 - \theta) \cdot \Delta x_D^{abs}] \cdot \frac{\partial}{\partial \tilde{x}} v(\tilde{x}, \tilde{y}) \Big|_{(\tilde{x}, \tilde{y})=(x-\varphi_x(j,0), y-\varphi_y(j,0))} \\
& \quad + [\theta \cdot \Delta y_0^{abs} - (1 - \theta) \cdot \Delta y_D^{abs}] \cdot \frac{\partial}{\partial \tilde{y}} v(\tilde{x}, \tilde{y}) \Big|_{(\tilde{x}, \tilde{y})=(x-\varphi_x(j,0), y-\varphi_y(j,0))} \\
& \quad + \theta \cdot \left[ \Delta x_0^{abs} \frac{\partial}{\partial \tilde{x}} n_0(\tilde{x}, \tilde{y}) \Big|_{(\tilde{x}, \tilde{y})=(x-\varphi_x(j,0), y-\varphi_y(j,0))} \right. \\
& \quad \quad \left. + \Delta y_0^{abs} \frac{\partial}{\partial \tilde{y}} n_0(\tilde{x}, \tilde{y}) \Big|_{(\tilde{x}, \tilde{y})=(x-\varphi_x(j,0), y-\varphi_y(j,0))} \right] \\
& \quad - (1 - \theta) \cdot \left[ \Delta x_D^{abs} \frac{\partial}{\partial \tilde{x}} n_D(\tilde{x}, \tilde{y}) \Big|_{(\tilde{x}, \tilde{y})=(x+\varphi_x(D,j), y+\varphi_y(D,j))} \right.
\end{aligned}$$

$$+ \Delta y_D^{abs} \frac{\partial}{\partial \tilde{y}} n_D(\tilde{x}, \tilde{y}) \Big|_{(\tilde{x}, \tilde{y})=(x+\varphi_x(D,j), y+\varphi_y(D,j))} \Big]$$

Let us derive an expression for the error autocorrelation.

$$\begin{aligned} R_{e_{j|0,D}^{absent}}(k, l) &= E \left\{ e_{j|0,D}^{absent}(x, y) \cdot e_{j|0,D}^{absent}(x+k, y+l) \right\} \\ &= \theta^2 \cdot R_{\Delta n_{j,0}}(k, l) + (1-\theta)^2 \cdot R_{\Delta n_{D,j}}(k, l) + \\ &\quad + \sigma_{\Delta x^{abs}}^2 \left[ \theta^2 + (1-\theta)^2 \right] \cdot autocorr \left\{ \frac{\partial}{\partial \tilde{x}} v(\tilde{x}, \tilde{y}) \Big|_{(\tilde{x}, \tilde{y})=(x-\varphi_x(j,0), y-\varphi_y(j,0))} \right\} \\ &\quad + \sigma_{\Delta y^{abs}}^2 \left[ \theta^2 + (1-\theta)^2 \right] \cdot autocorr \left\{ \frac{\partial}{\partial \tilde{y}} v(\tilde{x}, \tilde{y}) \Big|_{(\tilde{x}, \tilde{y})=(x-\varphi_x(j,0), y-\varphi_y(j,0))} \right\} \\ &\quad + \theta^2 \sigma_{\Delta x^{abs}}^2 \cdot autocorr \left\{ \frac{\partial}{\partial \tilde{x}} n_0(\tilde{x}, \tilde{y}) \Big|_{(\tilde{x}, \tilde{y})=(x-\varphi_x(j,0), y-\varphi_y(j,0))} \right\} \\ &\quad + \theta^2 \sigma_{\Delta y^{abs}}^2 \cdot autocorr \left\{ \frac{\partial}{\partial \tilde{y}} n_0(\tilde{x}, \tilde{y}) \Big|_{(\tilde{x}, \tilde{y})=(x-\varphi_x(j,0), y-\varphi_y(j,0))} \right\} \\ &\quad + (1-\theta)^2 \sigma_{\Delta x^{abs}}^2 \cdot autocorr \left\{ \frac{\partial}{\partial \tilde{x}} n_D(\tilde{x}, \tilde{y}) \Big|_{(\tilde{x}, \tilde{y})=(x-\varphi_x(D,j), y-\varphi_y(D,j))} \right\} \\ &\quad + (1-\theta)^2 \sigma_{\Delta y^{abs}}^2 \cdot autocorr \left\{ \frac{\partial}{\partial \tilde{y}} n_D(\tilde{x}, \tilde{y}) \Big|_{(\tilde{x}, \tilde{y})=(x-\varphi_x(D,j), y-\varphi_y(D,j))} \right\} \\ &\quad + \theta(1-\theta) E \{ \Delta n_{j,0}(x, y) \cdot \Delta n_{D,j}(x+\varphi_x(D,j)+k, y+\varphi_y(D,j)+l) \} \\ &\quad + \theta(1-\theta) E \{ \Delta n_{j,0}(x+k, y+l) \cdot \Delta n_{D,j}(x+\varphi_x(D,j), y+\varphi_y(D,j)) \} \end{aligned} \quad (69)$$

The cross-correlation between  $\Delta n_{j,0}$  and  $\Delta n_{D,j}$  is

$$E \{ \Delta n_{j,0}(x, y) \cdot \Delta n_{D,j}(x+\varphi_x(D,j)+k, y+\varphi_y(D,j)+l) \} = 0 \quad (70)$$

and

$$E \{ \Delta n_{j,0}(x+k, y+l) \cdot \Delta n_{D,j}(x+\varphi_x(D,j), y+\varphi_y(D,j)) \} = 0 \quad (71)$$

Setting (56), (70) and (71) into (69) results in

$$\begin{aligned} R_{e_{j|0,D}^{absent}}(k, l) &= \theta^2 \cdot R_{\Delta n_{j,0}}(k, l) + (1-\theta)^2 \cdot R_{\Delta n_{D,j}}(k, l) + \\ &\quad + \sigma_{\Delta x^{abs}}^2 \cdot \left[ \theta^2 + (1-\theta)^2 \right] \cdot [2R_v(k, l) - R_v(k-1, l) - R_v(k+1, l)] \\ &\quad + \sigma_{\Delta y^{abs}}^2 \cdot \left[ \theta^2 + (1-\theta)^2 \right] \cdot [2R_v(k, l) - R_v(k, l-1) - R_v(k, l+1)] \\ &\quad + \theta^2 \sigma_{\Delta x^{abs}}^2 \cdot [2R_{n_0}(k, l) - R_{n_0}(k-1, l) - R_{n_0}(k+1, l) \\ &\quad \quad + 2R_{n_D}(k, l) - R_{n_D}(k-1, l) - R_{n_D}(k+1, l)] \\ &\quad + \theta^2 \sigma_{\Delta y^{abs}}^2 \cdot [2R_{n_0}(k, l) - R_{n_0}(k, l-1) - R_{n_0}(k, l+1) \\ &\quad \quad + 2R_{n_D}(k, l) - R_{n_D}(k, l-1) - R_{n_D}(k, l+1)] \end{aligned} \quad (72)$$

According to (6),  $R_{n_t}$  is time-invariant; i.e., it does not depend on  $t$ . Hence,  $R_{n_0} \equiv R_{n_D}$  and (72) is simplified to

$$\begin{aligned}
R_{e_{j|0,D}^{absent}}(k, l) = & \theta^2 \cdot R_{\Delta n_{j,0}}(k, l) + (1 - \theta)^2 \cdot R_{\Delta n_{D,j}}(k, l) + \\
& + \sigma_{\Delta x^{abs}}^2 \cdot \left[ \theta^2 + (1 - \theta)^2 \right] \\
& \times [2R_v(k, l) - R_v(k - 1, l) - R_v(k + 1, l) \\
& \quad + 2R_{n_0}(k, l) - R_{n_0}(k - 1, l) - R_{n_0}(k + 1, l)] \\
& + \sigma_{\Delta y^{abs}}^2 \cdot \left[ \theta^2 + (1 - \theta)^2 \right] \\
& \times [2R_v(k, l) - R_v(k, l - 1) - R_v(k, l + 1) \\
& \quad + 2R_{n_0}(k, l) - R_{n_0}(k, l - 1) - R_{n_0}(k, l + 1)]
\end{aligned} \tag{73}$$

## References

- [1] B. Girod, “The efficiency of motion-compensating prediction for hybrid coding of video sequences,” *Selected Areas in Communications, IEEE Journal on*, vol. 5, no. 7, pp. 1140–1154, 1987.
- [2] —, “Efficiency analysis of multihypothesis motion-compensated prediction for video coding,” *Image Processing, IEEE Transactions on*, vol. 9, no. 2, pp. 173–183, 2000.
- [3] M. Flierl, T. Wiegand, and B. Girod, “Rate-constrained multihypothesis prediction for motion-compensated video compression,” *Circuits and Systems for Video Technology, IEEE Transactions on*, vol. 12, no. 11, pp. 957–969, 2002, iD: 2.
- [4] F. Kamisli and J. S. Lim, “Transforms for the motion compensation residual,” in *Acoustics, Speech and Signal Processing, 2009. ICASSP 2009. IEEE International Conference on*, 2009, pp. 789–792.
- [5] K.-C. Hui and W.-C. Siu, “Extended analysis of motion-compensated frame difference for block-based motion prediction error,” *Image Processing, IEEE Transactions on*, vol. 16, no. 5, pp. 1232–1245, 2007.
- [6] W. Niehsen and M. Brunig, “Covariance analysis of motion-compensated frame differences,” *Circuits and Systems for Video Technology, IEEE Transactions on*, vol. 9, no. 4, pp. 536–539, 1999.
- [7] C. F. Chen and K. K. Pang, “The optimal transform of motion-compensated frame difference images in a hybrid coder,” *Circuits and Systems II: Analog and Digital Signal Processing, IEEE Transactions on*, vol. 40, no. 6, pp. 393–397, 1993.
- [8] H. J. Leu, S.-D. Kim, and W.-J. Kim, “Statistical modeling of inter-frame prediction error and its adaptive transform,” *Circuits and Systems for Video Technology, IEEE Transactions on*, vol. 21, no. 4, pp. 519–523, 2011.
- [9] W. Zheng, Y. Shishikui, M. Naemura, Y. Kanatsugu, and S. Itoh, “Analysis of space-dependent characteristics of motion-compensated frame differences based on a statistical motion distribution model,” *Image Processing, IEEE Transactions on*, vol. 11, no. 4, pp. 377–386, 2002.
- [10] L. Guo, O. C. Au, M. Ma, Z. Liang, and P. Wong, “A novel analytic quantization-distortion model for hybrid video coding,” *Circuits and Systems for Video Technology, IEEE Transactions on*, vol. 19, no. 5, pp. 627–641, 2009.
- [11] C.-F. Chen and K. K. Pang, “Hybrid coders with motion compensation,” vol. 3, no. 2-3, pp. 241–266, 1992, j2: Multidim Syst Sign Process.

- [12] B. Tao and M. T. Orchard, "Prediction of second-order statistics in motion-compensated video coding," in *Image Processing, 1998. ICIP 98. Proceedings. 1998 International Conference on*, 1998, pp. 910–914 vol.3.
- [13] R. Feghali, F. Speranza, D. Wang, and A. Vincent, "Video quality metric for bit rate control via joint adjustment of quantization and frame rate," *Broadcasting, IEEE Transactions on*, vol. 53, no. 1, pp. 441–446, 2007.
- [14] Y. Zhang, D. Zhao, S. Ma, R. Wang, and W. Gao, "A motion-aligned autoregressive model for frame rate up conversion," *Image Processing, IEEE Transactions on*, vol. 19, no. 5, pp. 1248–1258, 2010.
- [15] J. Zhai, K. Yu, J. Li, and S. Li, "A low complexity motion compensated frame interpolation method," in *Circuits and Systems, 2005. ISCAS 2005. IEEE International Symposium on*, 2005, pp. 4927–4930 Vol. 5.
- [16] T. Q. Vinh, Y.-C. Kim, and S.-H. Hong, "Frame rate up-conversion using forward-backward jointing motion estimation and spatio-temporal motion vector smoothing," in *Computer Engineering and Systems, 2009. ICCES 2009. International Conference on*, 2009, pp. 605–609.
- [17] D. Wang, L. Zhang, and A. Vincent, "Motion-compensated frame rate up-conversionpart i: Fast multi-frame motion estimation," *Broadcasting, IEEE Transactions on*, vol. 56, no. 2, pp. 133–141, 2010.
- [18] D. Wang, A. Vincent, P. Blanchfield, and R. Klepko, "Motion-compensated frame rate up-conversionpart ii: New algorithms for frame interpolation," *Broadcasting, IEEE Transactions on*, vol. 56, no. 2, pp. 142–149, 2010.
- [19] G. Dane and T. Q. Nguyen, "Analysis of motion vector errors in motion compensated frame rate up conversion," in *Signals, Systems and Computers, 2003. Conference Record of the Thirty-Seventh Asilomar Conference on*, vol. 2, 2003, pp. 1534–1538 Vol.2.
- [20] [Online]. Available: <http://www.videolan.org/developers/x264.html>